PCCP

Accepted Manuscript

ROYAL SOCIETY OF CHEMISTRY

www.rsc.org/pccp

PCCP

ARTICLE

Effect of Graphene with Nanopore on Metal Clusters

*Hu Zhou[a], Xianlang Chen[a], Lei Wang[a], Xing Zhong[a], Guilin Zhuang[a], Xiaonian Li[a], Donghai Mei[b], Jianguo Wang[a]**

Received 00th January 20xx,
Accepted 00th January 20xx

DOI: 10.1039/x0xx00000x

www.rsc.org/

Porous graphene, which is a novel type of defective graphene, shows excellent potential as a support material for metal clusters. In this work, the stability and electronic structures of metal clusters (Pd, Ir, Rh) supported on pristine graphene and graphene with different sizes of nanopore were investigated by first-principle density functional theory (DFT) calculations. Thereafter, CO adsorption and oxidation reaction on the Pd-graphene system were chosen to evaluate its catalytic performance. Graphene with nanopore can strongly stabilize the metal clusters and cause a substantial downshift of the d-band center of the metal clusters, thus decreasing CO adsorption. All binding energies, d-band centers, and adsorption energies show a linear change with the size of the nanopore: a bigger size of nanopore corresponds to a stronger metal clusters bond to the graphene, lower downshift of the d-band center, and weaker CO adsorption. By using a suitable size nanopore, supported Pd clusters on the graphene will have similar CO and O_2 adsorption ability, thus leading to superior CO tolerance. The DFT calculated reaction energy barriers show that graphene with nanopore is a superior catalyst for CO oxidation reaction. These properties can play an important role in instructing graphene-supported metal catalyst preparation to prevent the diffusion or agglomeration of metal clusters and enhance catalytic performance.

Introduction

The interaction between the metal and support materials plays an important role in determining the stability and adsorption properties of catalysts, which lead to different activity and selectivity.[1-5] The property of metal nanoclusters is one of the major factors in determining catalytic performance.[6-9] However, the nature of support materials often has a substantial influence on the adsorption ability and catalytic activity of metal nanoclusters.[10] Metal oxide and carbon materials are two regularly employed supports.

Considerable efforts have been made to understand the effect of metal oxide on metal nanoclusters' catalysis ability since the pioneering work by Tauster *et al*.[11-16], who found that TiO_2 support can change the chemisorption abilities of Pt. Studies have also reported that Au supported on TiO_2, α-Fe_2O_3, and Co_3O_4 exhibit higher adsorption abilities for CO than isolated Au nanoclusters and can enhance its catalytic activities for low-temperature CO oxidation.[17-19] Furthermore, various studies have shown that metal nanoclusters over metal oxide supports possess better catalytic ability in reaction processes.[20-23] Our previous study provides a molecular understanding of why supported Au–Pt clusters over metal oxide show high performance for CO oxidation. One of the key factors is the stronger adsorption of O_2 on the supported catalyst than on isolated metal nanoclusters.[24]

In addition to metal oxides, carbon materials are also widely employed support materials. Graphene, carbon nanotubes (CNTs), and fullerene are expected as promising supports for noble metals with high areas, excellent structure stability, and non-toxicity. However, metal nanoclusters diffuse or agglomerate easily when adsorbed on perfect structures because of the low adsorption ability caused by the lack of anchoring sites on the supports.[25, 26] Several approaches have been proposed to solve this problem, such as by using oxygen-containing groups, nitrogen-containing groups, heteroatom-doped materials, and defective nanocarbon materials. Experiments have demonstrated that oxygen or nitrogen containing groups can stabilize metal nanoclusters and have better catalysis performance.[27-34] These studies by density functional theory (DFT) calculations, suggest that the enhanced binding between palladium clusters and surface functional groups (SFG)-modified carbon nanotubes (CNTs) follow the sequence CNTs–O > CNTs–OH > CNTs–COOH > CNTs.[32,35-37] Furthermore, for heteroatom-doped nanocarbon materials, various studies have confirmed that N, B, or other atom-substitution carbons effectively enhance the interaction between metal nanoclusters and carbon supports.[38-43] Defective carbon materials have been considered an excellent material as support.[44, 45] Experiments have also demonstrated that defects in graphene and CNTs can inhibit atom and cluster

[a] *College of Chemical Engineering, Zhejiang University of Technology, Hangzhou, 310032, P.R.China. E-mail: jgw@zjut.edu.cn. Fax:+86571-88871037; Tel: +86571-88871037*
[b] *Institute for Integrated Catalysis, Pacific Northwest National Laboratory, Richland, Washington 99352, USA.*
Electronic Supplementary Information (Additional tables and figures.). See DOI: 10.1039/x0xx00000x

diffusing effectively[46]; this finding is supported by theoretical studies.[47, 48] Recently, porous graphene, which is a special type of defective graphene, has been employed to achieve gas permeability.[49, 50] It also shows an excellent potential as the support to prevent diffusion and enhance the stabilization of the metal clusters. The application of porous graphene in supported metal catalyst has attracted considerable interests. An understanding of how the graphene with nanopore affect the stability, electronic structures, and adsorption ability of metal nanoclusters is beneficial for designing high performance graphene-supported metal catalysts.

There are plenty of theoretical studies have been made to investigate the behavior of metals on graphene.[51 52] However, to the best of our knowledge, no systematic study has been made on the effect of graphene with nanopore on metal nanoclusters' catalysis ability. In this work, by using first-principle DFT calculations, the stability and electronic structures of metals clusters (Pd, Ir, Rh) supported on pristine graphene and graphene with different size of nanopore were investigated. Then, CO adsorption and oxidation reaction on a Pd-graphene system were chosen to evaluate the catalytic performance. Our study shows that graphene with nanopore can enhance the stability of supported metal clusters and lead to a substantial downshift of the d-band center of metal clusters, thus further decreasing CO adsorption. The DFT-calculated reaction energy barriers demonstrate that Pd clusters supported on graphene with a suitable size of nanopore is a superior catalyst for CO oxidation reaction. Therefore, our study provides a theoretical perspective in the design of superior CO tolerance metal catalysts supported on graphene with nanopore.

Computational details

All calculations were performed by the plane-wave DFT method and implemented in the Vienna Ab-Initio Simulation Package (VASP).[53] The generalized gradient approximation (GGA) with Perdew–Burke–Ernzerhof (PBE)[54,55] formalism was used to treat the exchange–correlation effects. Transition states were located by the nudged elastic band (NEB) method.[56] All calculation were performed on a 6 × 6 graphene supercell with periodic boundary conditions were used with a 15 Å vacuum. A plane-wave basis set with a cutoff energy of 400 eV and ultrasoft Vanderbilt pseudopotentials (U.S.-PP) was employed. For metal-graphene system, the Brillouin zone integration was conducted with 4 × 4 × 1 k-point for geometry optimization and 6 × 6 × 2 k-point for electronic structure analysis. The convergence criterion of the force and energy is 10 meV $Å^{-1}$ and 0.1 meV. For isolated metal clusters, calculations were performed in a large supercell with Γ-point sampling only.

The binding energies (E_b) of Pd_4 clusters to the graphene substrate were calculated as follows:

$$E_b = E_{t(metal+C_m)} - E_{t(metal)} - E_{t(C_m)},$$

where $E_{t(metal+C_m)}$; $E_{t(metal)}$ and $E_{t(C_m)}$ are the total energies of the relaxed metal–graphene system, metal clusters, and graphene support. The adsorption energy (E_{ad}) of CO is defined as follows:

$$E_{ad} = E_{t(C_m+Pd_n+CO)} - E_{t(C_m+Pd_n)} - E_{t(CO)},$$

where $E_{t(C_m+Pd_n+CO)}$, $E_{t(C_m+Pd_n)}$, and $E_{t(CO)}$ are the total energies of the graphene–Pd_n–CO system, graphene–Pd_n system, and CO molecule as obtained from the DFT calculations.

Results and discussion

Enhanced Binding of Pd Clusters by Graphene Nanopore

The geometry optimizations of metal clusters supported on different graphene supports were performed first. The structures of Pd clusters supported on each support are shown in Figure 1, and the other two metals are displayed in Figure S2. Several graphene supports, such as pristine, vacancy, divacancies, trivacancies, and hexavacancies graphene, can be rendered to support metal clusters (Figure S1). Pd_n (n=3-8) clusters supported on five graphene supports can be written as Pd_n/G, Pd_n/GV1, Pd_n/GV2, Pd_n/GV3, Pd_n/GV6, respectively. Only the most and second most stable structures were shown. On pristine graphene, both the planar and tetrahedral structures of Pd_4 clusters are taken into account, with binding energies of −0.27 and −1.02 eV, respectively. Thus, the tetrahedral geometry was more strongly adsorbed on pristine graphene than the planar structure. This result is according

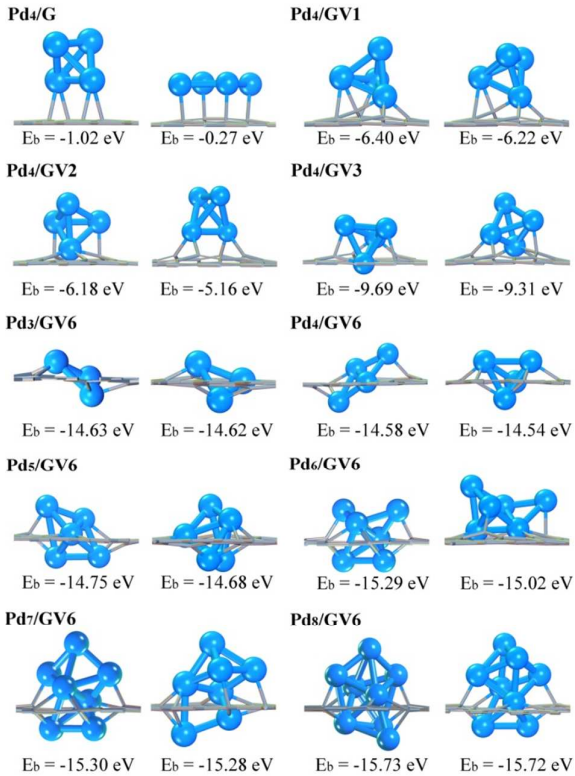

Figure 1. Optimized structures and binding energies of Pd_4/G, Pd_4/GV1, Pd_4/GV2, Pd_4/GV3, Pd_3/GV6, Pd_4/GV6, Pd_5/GV6, Pd_6/GV6, Pd_7/GV6, and Pd_8/GV6.

PCCP

ARTICLE

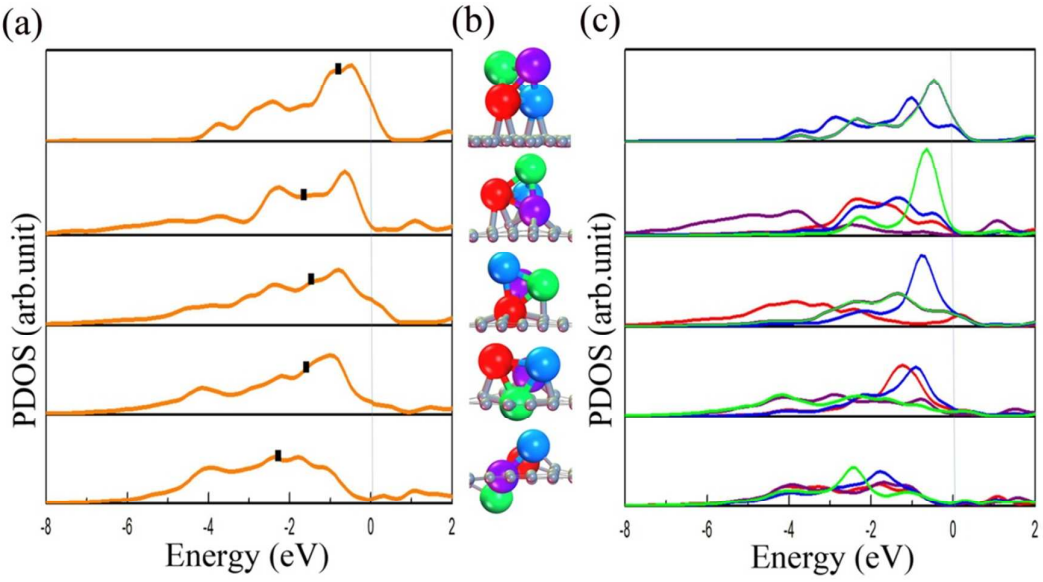

Figure 2. The PDOS of the most stable Pd_4 adsorption structures on each graphene supports (G, GV1, GV2, GV3, GV6). (a), PDOS of Pd_4 clusters (b), Relevant structures (c), PDOS of each Pd atoms.

well with previous study reported by Ioanna *et al*.[48] However, the contrary situation is exhibited on the hexavacancies graphene: the planar structure binds strongly by embedding into the nanopore, thus indicating that the geometrical configuration is affected by the nanopore. All the graphene with different size of nanopore exhibit stronger binding energies than pristine graphene, implying that graphene with nanopore possess better interactions with the supported metal cluster than pristine graphene. The binding energies of Pd_4 most strongly adsorbed on five graphene supports are −1.02, −6.40, −6.18, −9.69, and −14.58 eV, respectively. The absolute values of binding energies increase with the increasing size of the graphene nanopore. It indicates a general tendency that a lager nanopore leads to a stronger binding of Pd_4 on graphene supports. Other metals supported on graphene with nanopore also exhibit the same rules (Figure S2). Furthermore, a series of Pd_n(n=3-8) clusters on graphene with hexavacancies have been investigated. As shown in Figure 1, on the GV6, the binding energies of Pd_n(n=3-8) change slightly, changing from -14.63eV to 15.73eV. The nanopore on graphene can lead to strong binding of Pd clusters and big binding energies differences on various sites, thus can prevent the diffusion and agglomeration of metal clusters.[44,48,57-59]

Downshift of the d-Band Center of Pd Clusters by Graphene Nanopore

In addition to the enhanced binding of metal clusters by the graphene with nanopore, the electronic structures of metal clusters may also change, thus affecting the adsorption abilities and catalysis abilities. Therefore, the projected density of states (PDOS) of Pd_4 clusters supported on each support were investigated (Figure 2). The d-band of Pd_4 clusters supported on graphene with nanopore (Figure 2a, b) substantially move downshift compared with that supported on pristine graphene. The shifts in the Pd d-band were quantified by determining the position of the d-band center (black points in the Figure 2a) of the adsorbed cluster. The values of the d-band center of Pd clusters (Pd_4/G, Pd_4/GV1, Pd_4/GV2, Pd_4/GV3, Pd_4/GV6) are −0.77, −1.67, −1.47, −1.58 and −2.29 eV, respectively. It indicates a bigger nanopore size corresponds to more downshifts in the d-band center. Figure 2c shows the PDOS of each Pd atom, in which the color is same with the relevant Pd atom (Figure 2b). The PDOS of Pd atoms on pristine graphene can be divided into two groups, one group belongs to the Pd atoms directly bond to the graphene

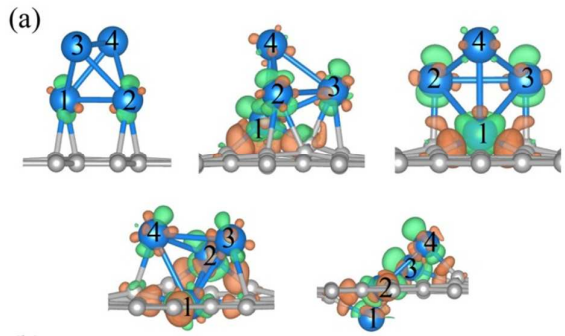

(b)

Atoms	Charge (e)				
	Pd(G)	Pd(GV1)	Pd(GV2)	Pd(GV3)	Pd(GV6)
1	0.12	0.36	0.40	0.38	0.22
2	0.12	0.08	0.09	0.20	0.20
3	-0.07	0.08	0.09	0.07	0.20
4	-0.07	-0.21	-0.08	0.07	0.13
Total	**0.10**	**0.31**	**0.5**	**0.72**	**0.75**

Figure 3. (a) Charge density differences induced by the Pd_4 cluster on each graphene supports (G, GV1, GV2, GV3, GV6); (b) charge of relevant Pd atoms.

and another group belongs to the Pd atoms on the second layer. However, when Pd_4 is supported on graphene with nanopore, each Pd atom shows different PDOS properties, which indicates that the pronounced electronic properties change of Pd nanoclusters when they bond with the carbon of graphene nanopore. These results may explain that why the downshifts of the d-band center of the Pd clusters are linearly correlative to the size of the nanopore. More Pd atoms that bind to the carbon of graphene nanopore lead to the lower downshift of the d-band center of Pd clusters.

The charge density changes induced by Pd_4 on graphene with nanopore and on pristine graphene are shown in Figure 3a. The positive charging state (brown isosurfaces) of Pd atoms directly bonding with graphene nanopore is obvious, whereas the positive charging state of Pd_4 on pristine graphene is small. It indicates that the graphene with nanopore definitely change the electronic structures of Pd. The overall features show that a bigger nanopore size corresponds to more charge transfer. To quantity the total charge transfer, Bader analysis was performed on the most stable structures, which are listed in Figure 3b. From the data of each row, it was found a bigger size of nanopore corresponds to more electron transfer from Pd atoms to graphene with nanopore. Which was more clearly exhibited by the total charge of Pd_4 clusters, while the charge changing from +0.10 to +0.75e. The data of each column show that the positive charge of each Pd atoms increase as Pd atoms close to the support. It indicates that the more bonds between Pd atom and graphene with nanopore corresponds to the more charge transfer from Pd to the support.

To further understand the change of electronic structures

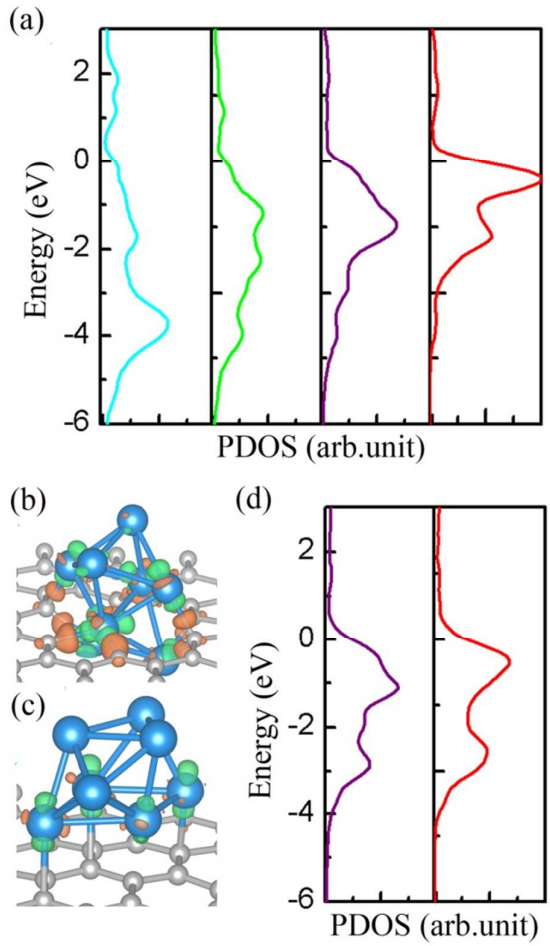

Figure 4. The PDOS and charge density differences of Pd_8/GV6 and Pd_8/G. (a) PDOS of Pd(four groups) on GV6; (b), (c) Charge density differences induced by the Pd_8 cluster on GV6 and G; (d) PDOS of Pd(two groups) on G.

with the distance between Pd clusters and graphene nanopore, the density of states of larger Pd clusters (Pd_8) on two types of graphene and charge density differences were analyzed. The PDOS of Pd atoms on graphene with nanopore defects can be divided into four groups according to the distance between Pd atoms and graphene support(Figure 4a), in which the shorter distance between carbon and Pd, the lower d-band center of Pd. However, when the Pd_8 cluster is supported on the pristine graphene (Figure 4d), only the d-band center of the Pd directly bonding with graphene slightly move downwards compared with the Pd that on the second layer. The charge density change induced by Pd_8 on graphene with nanopore and pristine graphene are shown in Figures 4b and c. The positive charging state (brown isosurfaces) of the 1st layer Pd atoms directly bonding to graphene with nanopore defects is obvious. By contrast, Pd_8 on pristine graphene has very small charge. The total charge of Pd_8 (Figure S3) on graphene with nanopore and pristine graphene is +1.24

and +0.42 e, respectively. The results show that Pd atoms closer to the graphene nanopore

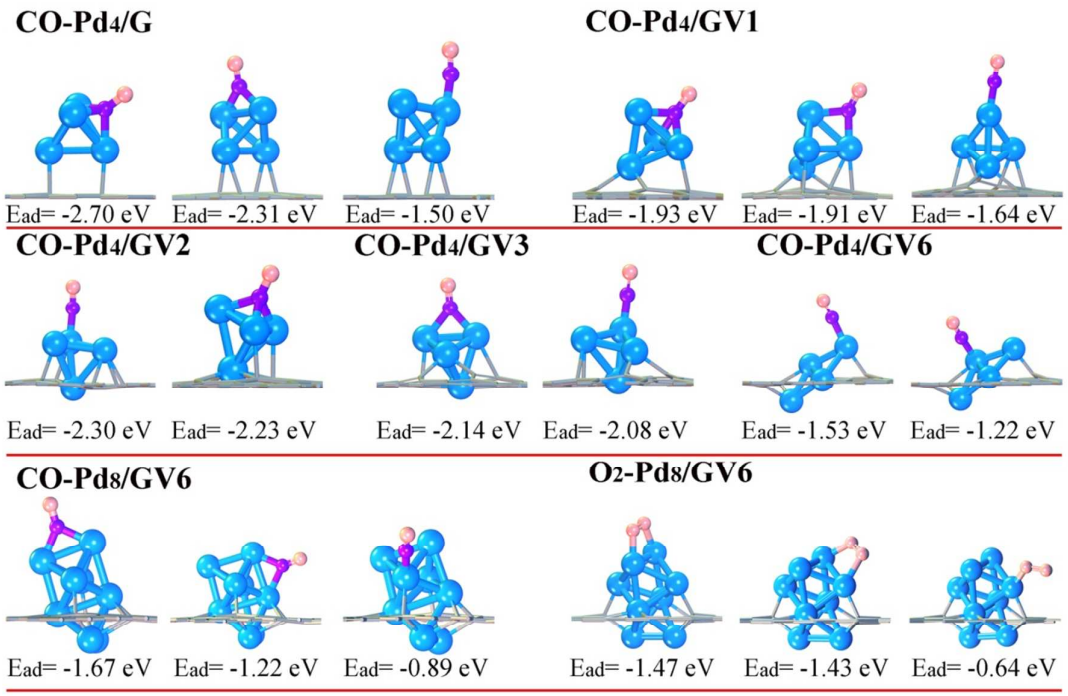

Figure 5. Optimized structures and E_{ad}(CO, O_2) on the most stable structures: CO–Pd_4/G, CO–Pd_4/GV1, CO–Pd_4/GV2, CO–Pd_4/GV3, CO–Pd_4/GV6, CO–Pd_8/GV6, O_2–Pd_8/GV6.

correspond to more change of electronic structures.

The d-band center, the charge density difference and Bader charge analysis show that the graphene with nanopore greatly changes the electronic structure of the Pd cluster because of the charge transfer between the Pd clusters and the supports. The graphene with nanopore can lead to a downshift of the d-band center. This result can also be found in the PDOS of Ir_4-graphene and Rh_4-graphene systems (Figure S4). Further analysis indicates that a bigger nanopore leads to more changes of electronic structure, including the d-band center, charge density, and Bader charge. All of these changes of electronic structures may change the adsorption abilities and catalytic performance of metal clusters.

Weak CO Adsorption on Pd Clusters by Graphene Nanopores

The modification of electronic properties of Pd clusters by graphene with nanopore may also play an important role on the adsorption and catalytic properties. The interface between Au and TiO_2 can enhance O_2 adsorption and CO oxidation abilities because of the charge transfer between Au and TiO_2.[24, 57] However, we found that in contrast to Au-supported TiO_2 systems, CO adsorption on Pd-graphene with nanopore (Figure 5) becomes weaker than that on Pd surfaces and Pd clusters supported on pristine graphene. As a probe molecule, CO is chosen to investigate the adsorption of Pd-graphene systems. A variety of adsorption modes on the Pd clusters, including bridge, top, and hollow, were detected. The optimized structures and calculated CO adsorption energies were summarized in Figure 5. When CO adsorbed on the isolated Pd_4 cluster, the most stable site is hollow site and the adsorption energy is −2.70 eV (Figure S5), similar with the E_{ad} of CO when most strongly adsorbed on Pd_4/G. However, all of the adsorption energies of CO adsorbed on Pd_4 supported on graphene with nanopore are smaller than −2.70 eV. This result indicates that graphene with nanopore can reduce the adsorption ability of Pd_4 clusters for CO, thus indicating that graphene with nanopore can enhance the CO tolerance of Pd_4 clusters. By comparing the adsorption energies of the most strongly adsorbed CO on each structure, we found that the adsorption energies of CO exhibit a decreasing trend with increasing nanopore size; the adsorption energies are −2.70, −1.93, −2.30, −2.14 and −1.53 eV, respectively.

One of the key problems in CO oxidation reaction is the poisoning of noble metal catalyst. The main reason is that the difference of adsorption between CO and O_2 is large, whereas the adsorption of CO on noble clusters is too strong and the adsorption of O_2 is weak. Thus, CO and O_2 adsorptions on Pd_8/GV6 catalysts were further analyzed. The results show that Pd_8/GV6 have similar adsorption abilities for CO and O_2 (Figure 5), which can enhance the CO tolerance of Pd clusters. There seems to be a relation between CO adsorption energies, binding energies, d-band center, and nanopore size, we attempted to make it clear. It is well known that CO adsorption energies linearly increase with the downshift of d-band center (Figure 6a).[60,61] Besides, CO adsorption abilities of the Pd_4-PGra

system exhibit a decreasing trend with increasing energies of Pd clusters on graphene increase with the size of nanopore.

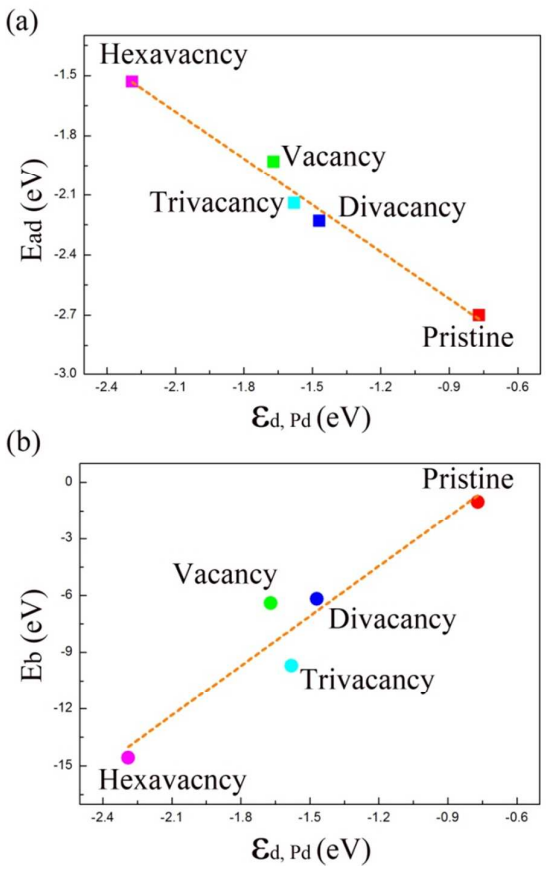

Figure 6. The linear relation between d-band center (ε_d,Pd) and (a) adsorption energies (E_{ad}) of CO; (b) binding energies (E_b) of Pd_4 clusters.

Interestingly, we found that there is a linear relation between the binding energies and d-band center of metal clusters.

CO Oxidation on Pd Clusters Supported on Graphene Nanopore

The further study of reaction mechanism was performed. Figure 7 shows DFT-calculated catalytic cycles for CO oxidation on Pd_8/Graphene with nanopore. First, CO and O_2 co-adsorption energies are present, wherein the adsorption strength of O_2 is similar to that of CO (I). O_2 disassociates into atomic oxygen with moderate activation energies (0.51 eV), and the atomic oxygen is adsorbed on hollow and bridge site (II). Once the atomic oxygen is obtained (III), CO easily reacts with the atomic oxygen with 0.49 eV reaction barriers (IV). CO releases approximately −3.35 eV when CO_2 first forms. The remaining oxygen may easily be removed by the second adsorbed CO (V) with +0.48 eV activation energy (VI), thereby forming CO_2 and closing the cycle. The reaction route calculated by DFT shows that Pd supported on graphene with nanopore may be a superior catalyst for CO oxidation.

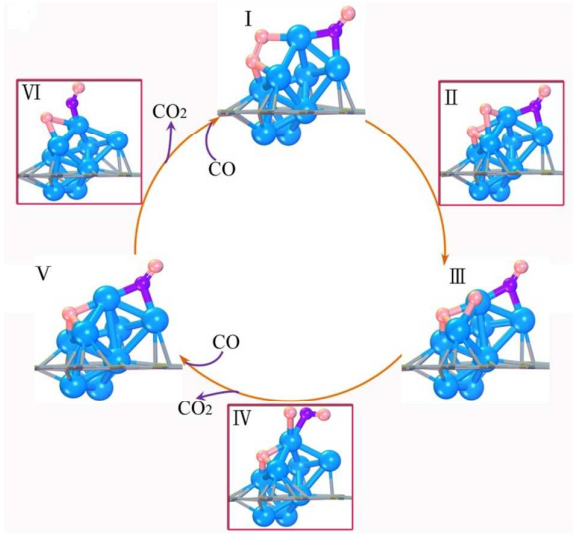

Figure 7. Reaction cycle for CO oxidation over Pd_8/GV6

Conclusion

The structures, properties of small noble metal clusters supported on pristine graphene and graphene with different size of nanopore were investigated by means of DFT calculations. It was found that graphene with nanopore can enhance the stability of metal clusters. The binding energies of Pd clusters on graphene linearly increase with the size of nanopore. There is a linear relation between the binding energies and d-band center of metal clusters. Especially, graphene with nanopore can lead to the substantial downshift of d-band center of metal clusters, which further decrease the adsorption for CO. The d-band center linearly move downshift with increasing the size of nanopore. The adsorption energies of CO are linearly correlative to the d-band center of metal clusters. Importantly, graphene with suitable nanopore will lead to the similar CO and O_2 adsorption ability on Pd clusters, which may act as the superior CO tolerance catalyst. Indeed, DFT calculated the reaction barriers for CO oxidation on such clusters is small. These remarkable characteristics suggested that graphene with nanopore supported metal nanoclusters will act as one novel advanced catalysts for a series of applications.

Acknowledgements

This work was supported by National Basic Research Program of China (973Program) (2013CB733501), the National Natural Science Foundation of China (NSFC-21176221, 21136001, 21101137, 21306169, and 91334013).

Notes and references

1. B. T. Qiao, A. Q. Wang, X. F. Yang, L. F. Allard, Z. Jiang, Y. T. Cui, J. Y. Liu, J. Li and T. Zhang, *Nature Chem.*, 2011, **3**, 634-641.
2. S. Pérez-Rodríguez, N. Rillo, M. J. Lázaro and E. Pastor, *Appl Catal B-Environ*, 2015, **163**, 83-95.
3. J. Martins, N. Batail, S. Silva, S. Rafik-Clement, A. Karelovic, D. P. Debecker, A. Chaumonnot and D. Uzio, *Catal. Commun.*, 2015, **58**, 11-15.
4. K. Liu, X. Yan, P. Zou, Y. Wang and L. Dai, *Catal. Commun.*, 2015, **58**, 132-136.
5. G. Portale, L. Sciortino, C. Albonetti, F. Giannici, A. Martorana, W. Bras, F. Biscarini and A. Longo, *Phys. Chem. Chem. Phys.*, 2014, **16**, 6649-6656.
6. S. Kunz, F. F. Schweinberger, V. Habibpour, M. Rottgen, C. Harding, M. Arenz and U. Heiz, *J. Phys. Chem. C*, 2010, **114**, 1651-1654.
7. A. S. Worz, K. Judai, S. Abbet and U. Heiz, *J. Am. Chem. Soc.*, 2003, **125**, 7964-7970.
8. D. Gao, H. Zhou, J. Wang, S. Miao, F. Yang, G. Wang, J. Wang and X. Bao, *J. Am. Chem. Soc.*, 2015, **137**, 4288-4291.
9. I. V. Yudanov, A. Genest, S. Schauermann, H. J. Freund and N. Rosch, *Nano Lett.*, 2012, **12**, 2134-2139.
10. J. K. Edwards, A. Thomas, B. E. Solsona, P. Landon, A. F. Carley and G. J. Hutchings, *Catal. Today*, 2007, **122**, 397-402.
11. M. M. Schubert, S. Hackenberg, A. C. van Veen, M. Muhler, V. Plzak and R. J. Behm, *J. Catal.*, 2001, **197**, 113-122.
12. A. Bruix, J. A. Rodriguez, P. J. Ramirez, S. D. Senanayake, J. Evans, J. B. Park, D. Stacchiola, P. Liu, J. Hrbek and F. Illas, *J. Am. Chem. Soc.*, 2012, **134**, 8968-8974.
13. M. Cargnello, V. V. T. Doan-Nguyen, T. R. Gordon, R. E. Diaz, E. A. Stach, R. J. Gorte, P. Fornasiero and C. B. Murray, *Science*, 2013, **341**, 771-773.
14. P. P. Hu, Z. W. Huang, Z. Amghouz, M. Makkee, F. Xu, F. Kapteijn, A. Dikhtiarenko, Y. X. Chen, X. Gu and X. F. Tang, *Angew. Chem. Int. Ed.*, 2014, **53**, 3418-3421.
15. S. J. Tauster, S. C. Fung and R. L. Garten, *J. Am. Chem. Soc*, 1978, **100**, 170.
16. B. Chai, T. Y. Peng, J. Mao, K. Li and L. Zan, *Phys. Chem. Chem. Phys.*, 2012, **14**, 16745-16752.
17. M. Haruta, S. Tsubota, T. Kobayashi, H. Kageyama, M. J. Genet and B. Delmon, *J. Catal.*, 1993, **144**, 175-192.
18. M. Haruta, *Gold Bull.*, 2004, **37**, 27-36.
19. P. Kast, G. Kučerová and R. J. Behm, *Catal. Today*, 2015, **244**, 146-160.
20. J. Scott, W. Irawaty, G. Low and R. Amal, *Appl Catal B-Environ*, 2015, **164**, 10-17.
21. V. Choque, P. R. de la Piscina, D. Molyneux and N. Homs, *Catal. Today*, 2010, **149**, 248-253.
22. S. C. Parker and C. T. Campbell, *Phys. Rev. B*, 2007, **75**, 15.
23. Tana, F. G. Wang, H. J. Li and W. J. Shen, *Catal. Today*, 2011, **175**, 541-545.
24. Q. Cai, X. Wang and J.-g. Wang, *J. Phys. Chem. C*, 2013, **117**, 21331-21336.
25. Y. J. Gan, L. T. Sun and F. Banhart, *Small*, 2008, **4**, 587-591.
26. B. H. Morrow and A. Striolo, *Nanotechnology*, 2008, **19**, 10.
27. I. D. Rosca, F. Watari, M. Uo and T. Akaska, *Carbon*, 2005, **43**, 3124-3131.
28. N. Y. Zhang, J. Me and V. K. Varadan, *Smart Mater. Struct.*, 2002, **11**, 962-965.
29. M. Carmo, M. Linardi and J. G. R. Poco, *Int. J. Hydrogen Energy*, 2008, **33**, 6289-6297.
30. A. E. Aksoylu, J. L. Faria, M. F. R. Pereira, J. L. Figueiredo, P. Serp, J. C. Hierso, R. Feurer, Y. Kihn and P. Kalck, *Appl Catal a-Gen*, 2003, **243**, 357-365.
31. X. Zhong, H. Yu, G. Zhuang, Q. Li, X. Wang, Y. Zhu, L. Liu, X. Li, M. Dong and J.-g. Wang, *J. Mater. Chem. A*, 2014, **2**, 897-901.
32. T.-y. Xu, Q.-f. Zhang, H.-f. Yang, X.-n. Li and J.-g. Wang, *Ind. Eng. Chem. Res.*, 2013, **52**, 9783-9789.
33. Y. Li, Y. Yu, J.-G. Wang, J. Song, Q. Li, M. Dong and C.-J. Liu, *Appl Catal B-Environ*, 2012, **125**, 189-196.
34. D. Ma, S. Jia, D. Zhao, Z. Lu and Z. Yang, *Appl. Surf. Sci.*, 2014, **300**, 91-97.
35. X. Wang, Q. Cai, G. Zhuang, X. Zhong, D. Mei, X. Li and J. Wang, *Phys. Chem. Chem. Phys.*, 2014, **16**, 20749-20754.
36. S.-Y. Wu and J.-J. Ho, *J. Phys. Chem. C*, 2014, **118**, 26764-26771.
37. K. Xu and P. D. Ye, *J. Phys. Chem. C*, 2014, **118**, 10400-10407.
38. Q. L. Williams, X. Liu, W. Walters, J. G. Zhou, T. Y. Edwards and F. L. Smith, *Appl. Phys. Lett.*, 2007, **91**, 3.
39. X. M. Liu, H. E. Romero, H. R. Gutierrez, K. Adu and P. C. Eklund, *Nano Lett.*, 2008, **8**, 2613-2619.
40. D. H. Lee, W. J. Lee and S. O. Kim, *Nano Lett.*, 2009, **9**, 1427-1432.
41. Y. Gao, G. Hu, J. Zhong, Z. Shi, Y. Zhu, D. S. Su, J. Wang, X. Bao and D. Ma, *Angew. Chem., Int. Ed.*, 2013, **52**, 2109-2113.
42. D. S. Geng, S. L. Yang, Y. Zhang, J. L. Yang, J. Liu, R. Y. Li, T. K. Sham, X. L. Sun, S. Y. Ye and S. Knights, *Appl. Surf. Sci.*, 2011, **257**, 9193-9198.
43. N. Jung, B. Kim, A. C. Crowther, N. Kim, C. Nuckolls and L. Brus, *ACS Nano*, 2011, **5**, 5708-5716.
44. J. G. Wang, Y. A. Lv, X. N. Li and M. D. Dong, *J. Phys. Chem. C*, 2009, **113**, 890-893.
45. J. V. Zoval, J. Lee, S. Gorer and R. M. Penner, *J. Phys. Chem. B*, 1998, **102**, 1166-1175.
46. J. A. Rodriguez-Manzo, O. Cretu and F. Banhart, *ACS Nano*, 2010, **4**, 3422-3428.
47. I. Fampiou and A. Ramasubramaniam, *J. Phys. Chem. C*, 2012, **116**, 6543-6555.
48. I. Fampiou and A. Ramasubramaniam, *J. Phys. Chem. C*, 2013, **117**, 19927-19933.
49. D. E. Jiang, V. R. Cooper and S. Dai, *Nano letters*, 2009, **9**, 4019-4024.
50. Y. H. Tao, Q. Z. Xue, Z. L. Liu, M. X. Shan, C. C. Ling, T. T. Wu and X. F. Li, *ACS Appl. Mater. Interfaces*, 2014, **6**, 8048-8058.
51. Z. E. Hughes, T. R. Walsh, *Nanoscale*, 2015, **7**, 6883-6908.
52. T. X. Zhang, Q. Z. Xue, S. Zhang, M. D. Dong, *Nano Today*, 2012, **7**, 180-200.
53. G. Kresse and D. Joubert, *Phys. Rev. B*, 1999, **59**, 1758-1775.
54. J. P. Perdew, K. Burke and M. Ernzerhof, *Phys. Rev. Lett.*, 1997, **78**, 1396-1396.

55. B. Delley, *J. Chem. Phys.*, 2000, **113**, 7756-7764.
56. G. Henkelman, H. Jonsson, *J. Chem. Phys.* 2000, **113** (22), 9978–9985.
57. D. Matthey, J. G. Wang, S. Wendt, J. Matthiesen, R. Schaub, E. Laegsgaard, B. Hammer, F. Besenbacher, *Science*, 2007, **315**, 1692-1696.
58. Y. A. Lv, Y. H. Cui, X. N. Li, X. Z. Song, J. G. Wang, M. D. Dong, *Physica E*, 2010, **42**, 1746–1750.
59. J. H. Xu, J. Zhao, J. T. Xu, T. T. Zhang, X. N. Li, X. X. Di, J. Ni, J. G. Wang, J. Cen. *Ind. Eng. Chem. Res*. 2014, **53**, 14272−14281.
60. M. Mavrikakis, B. Hammer, J. K. Nørskov, *Physical Review Letters*, 1998, **81**, 2819.
61. J. R. Kitchin, J. K. Norskov, M. A. Barteau, *J. Phys. Chem. C,* 2004, **120**, 10240-10246.